Numerical simulation of an infinite array of airfoils with a finite span

Takahiro Ikeda[1], Masashi Yamakawa[1], Shinichi Asao[2], Seiichi Takeuchi[2]

[1] Kyoto Institute of Technology, Matsugasaki, Sakyo-Ku, Kyoto, 606-8585 Japan
[2] College of Industrial Technology, 1-27-1 Amagasaki, Hyogo, 661-0047, Japan

Abstract. Fish and birds can propel themselves efficiently by acting in groups and clarifying their hydrodynamic interactions will be very useful for engineering applications. In this study, concerning the work of Becker et al., we performed three-dimensional unsteady simulations of an infinite array of airfoils, which is one of the models of schooling, and we clarified the structure of the flow between them. The model velocities obtained from the simulations show a good correspondence with the experimental data of Becker et al. The vortex structure created by the airfoil is very complicated, and it is visually clear that the vortices generated from the left and right ends of the airfoil also contribute to the formation of the upward and downward flows.

Keywords: Computational Fluid Dynamics, Flapping airfoil, self-propulsion

1 Introduction

Fish and birds can propel themselves by periodically moving or morphing their body. Many researchers and experts have conducted experiments and numerical simulations for oscillating airfoils to understand the propulsion mechanism hidden in their behavior [1]. In addition, it is known that migratory birds and small fishes such as sardines can travel with high energy efficiency by forming schools [2]. Inspired by them, Becker et al. [3] investigated the fluid-mediated interactions among the collective locomotion of self-propelled bodies through experiments and numerical simulations of array of flapping airfoils. In their study, the system was numerically calculated as the horizontal translational system of two-dimensional array of airfoils, since it is known that it shows a good comparison with the rotational system. Although it might be true, the flow structure of the three-dimensional array should be different from the two-dimensional one. The flow structure and the properties of the horizontal array of flapping airfoils with finite spans is still unclear.

Our research aims to clarify the flow structure of the three-dimensional horizontal array of flapping airfoils numerically. In this paper, the Moving-Grid Finite-Volume Method was adopted [4-5]. This method can satisfy the physical conservation laws while moving or morphing the grids, so it is suitable for our study. To realize the self-propelled body in the simulation, we also adopt the concept of the Moving Computational Domain (MCD) method [6] .

ICCS Camera Ready Version 2022
To cite this paper please use the final published version:
DOI: 10.1007/978-3-031-08760-8_27

2 Simulation

2.1 Governing equations

As the governing equations, the incompressible Navier Stokes (NS) equations are adopted. They are expressed as

$$\frac{\partial \mathbf{Q}}{\partial t}+\frac{\partial \mathbf{E}_c+\mathbf{E}_v}{\partial x}+\frac{\partial \mathbf{F}_c+\mathbf{F}_v}{\partial y}+\frac{\partial \mathbf{G}_c+\mathbf{G}_v}{\partial z}=\mathbf{0}, \tag{1}$$

where

$$\mathbf{Q}=\begin{bmatrix}u\\v\\w\end{bmatrix},\mathbf{E}_c=\begin{bmatrix}u^2+p\\vu\\wu\end{bmatrix},\mathbf{F}_c=\begin{bmatrix}uv\\v^2+p\\wv\end{bmatrix},\mathbf{G}_c=\begin{bmatrix}uw\\vw\\w^2+p\end{bmatrix}, \tag{2}$$

$$\mathbf{E}_{\mathrm{v}}=-\frac{1}{\mathrm{Re}}\begin{bmatrix}\partial u/\partial x\\\partial v/\partial x\\\partial w/\partial x\end{bmatrix},\mathbf{F}_{\mathrm{v}}=-\frac{1}{\mathrm{Re}}\begin{bmatrix}\partial u/\partial y\\\partial v/\partial y\\\partial w/\partial y\end{bmatrix},\mathbf{G}_{\mathrm{v}}=-\frac{1}{\mathrm{Re}}\begin{bmatrix}\partial u/\partial z\\\partial v/\partial z\\\partial w/\partial z\end{bmatrix}. \tag{3}$$

Here, the variables u, v, w are velocity and p is pressure.
Also, the mass conservation law is written as

$$\frac{\partial u}{\partial x}+\frac{\partial v}{\partial y}+\frac{\partial w}{\partial z}=0. \tag{4}$$

The governing equations shown above are nondimensionalized using the characteristic length c, velocity U_∞, density ρ_∞ and viscosity μ_∞. The Reynolds number becomes

$$\mathrm{Re}=\frac{\rho_\infty U_\infty c}{\mu_\infty}. \tag{5}$$

Here, $c = 0.06$ m is a cord length of the airfoil. $U_\infty = 0.1$ m/s, and the viscosity and the density are $\rho_\infty = 1000.0$ kg/m^{3}and $\mu_\infty = 0.001$ Pa$\cdot$s, referring to the values in [3].

2.2 Numerical Approach

In this study, the moving-grid finite-volume method [4-5] is used to solve the flow field with a moving object. In this method, the governing equations are integrated and discretized in a four-dimensional control volume of a unified space and time domain, so that the conservation law can be satisfied even when the grid is moving or deformed. In this study, we apply this method to the unstructured grid using cell-centered and collocated arrangement. In addition, the MCD method [6] is applied to analyze the free propulsion of an airfoil in this paper. To solve the incompressible NS equation discretized by the above method, the Fractional Step method [7] is adopted in this study. To solve the linear system of equations for both steps, the Lower-Upper Symmetric Gauss Seidel (LU-SGS) method [8] is used for the pseudo velocity and the

ICCS Camera Ready Version 2022
To cite this paper please use the final published version:
DOI: 10.1007/978-3-031-08760-8_27

Successive Over Relaxation (SOR) method is used for the pressure equations. All computations in this paper are conducted by in-house code.

2.3 Computational model

The model simulated in this paper is an array of equally spaced airfoils in a row. In the numerical simulation of [3], the array is realized by a single flapping airfoil with periodic boundary conditions. In this paper, we also compute the similar one to the computation, but the difference is that the flow domain is three-dimensional, and the wing has a finite span length. Then, our computational model is shown in Fig.1. The coordinate axes are x for the direction opposite to the airfoil's direction of motion, y for the direction of vibration, and z for the rest. The shape of the airfoil is NACA(National Advisory Committee for Aeronautics)0017 which has a chord length of c = 0.06 m and a span length of 0.15m. These dimensions are the same as in the experiment. The flow region has a length of $4c$ in span-wise direction, and the same lengths as the numerical simulation [3] in stream-wise and vertical direction.

The airfoil is given a prescribed vertical motion written in the dimensionless form as

$$y(t) = -\frac{A}{2c}\sin(2\pi f t), \tag{6}$$

where the amplitude is $A = 0.09$m and the f is a nondimensionalized frequency defined as

$$f = \frac{\bar{f}c}{U_\infty}. \tag{7}$$

The frequency varies in the range $0.1 \leq \bar{f} \leq 0.3$ Hz.

The propulsive force of the airfoil is calculated by integrating the viscous and pressure force acted on the surface. Using the force, propulsive velocity is determined by the Newton's second law described as

$$\rho V \frac{dv_{wing}}{dt} = F_{thrust}, \tag{8}$$

where $\rho = \rho_{wing}/\rho_\infty$. $\rho_{wing} = 10\rho_\infty$ is the density of the airfoil. V is the volume of the airfoil. The airfoil is fixed in the span-wise direction so that it can move only in the propulsive and vertical directions, therefore the dynamical motion of the airfoil is determined only by equation (6) and (8).

ICCS Camera Ready Version 2022
To cite this paper please use the final published version:
DOI: 10.1007/978-3-031-08760-8_27

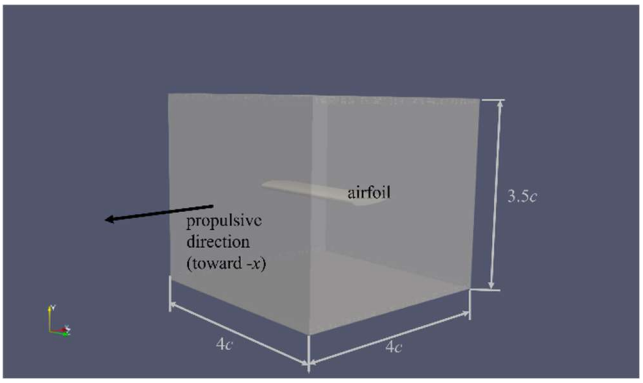

Fig. 1. The three-dimensional model for this study. the wing and the flow domain move toward the negative x direction with flapping in vertical (yellow axis in the figure) direction.

As for the boundary conditions, no-slip conditions are imposed on the blade surfaces, fixed velocity conditions ($\mathbf{u} = 0$) are upper and lower walls, and symmetric conditions are imposed on the sides. For inflow and outflow, periodic boundary conditions are used to reproduce a model with an infinite array of airfoils. All pressures are set to zero gradients, and the mean value of the pressures is fixed for the simulation.

Based on the above model, a spatial grid was created as follows. Fig.2 shows a cross section of the unstructured grid used in this study. MEGG3D [9] was used to create the unstructured grid for the computation. The number of elements is 2,879,012. Prismatic layers are created on the surface of the airfoil and upper and lower walls. The minimum grid width is wide enough to capture the viscous sublayer, and the number of layers is 17 to reduce the size ratio to the tetra grid. All dimensions are nondimensionalized.

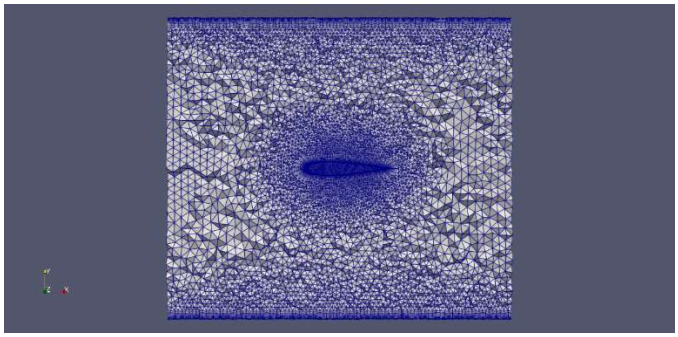

Fig. 2. Cross section of the unstructured grid for the computation of flapping airfoil.

3 Results

Fig.3 shows a comparison of the propulsive velocity calculated as described above with that of the experiment in [3], where the amplitude is $A = 0.1$m. Since the origi-

ICCS Camera Ready Version 2022
To cite this paper please use the final published version:
DOI: 10.1007/978-3-031-08760-8_27

nal data in the experiment is expressed in terms of rotational frequency F[1/s], it is necessary to convert it to translational velocity for comparison. In this study, based on the dimensions of the water tank in the experiment in [3], the reference value of the propulsive velocity is calculated as follows,

$$v = 2\pi RF. \tag{5}$$

In equation (5), R=26cm is a distance from the axis of rotation to the mass center of each airfoil. From the figure, it can be seen that the speed of progression in the literature [3] and that in this study are in good agreement, although the amplitudes and the flow geometries are different. It is mentioned that the flows observed in rotational geometry compare well with those in translational one [3,10], therefore it can be said that our result is also true.

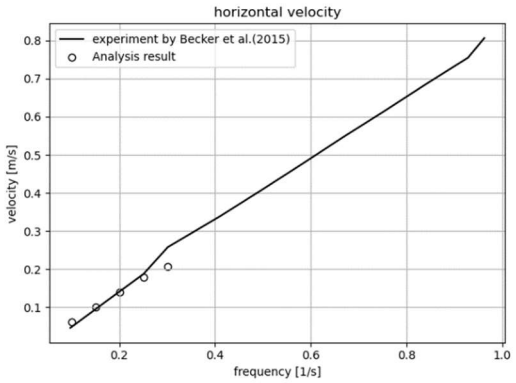

Fig. 3. The horizontal velocity of the airfoils. white circles are current results, and a solid line is the result by Becker et al.

Next, we describe the flow field. The isosurfaces of the Q-criterion are shown in Fig. 4 to clarify the vortex structure. The Q criterion is the second invariant of the velocity gradient tensor, and the region of $Q > 0$ is often used to identify vortices in the flow [11]. The color indicates the x component of the vorticity. In the figure, the airfoil is descending to the lower wall. Many vortices are generated in the spanwise direction of the airfoil surface, and these vortices form a large vortex at the trailing edge, but their shape is curved and not straight. The vortices generated by the airfoil are not only in the spanwise direction but also in the direction of motion. Since the airfoil is moving in the negative direction of x as it descends, the blue vortex on the left side of the airfoil has the same direction as the direction of motion, and the red vortex on the right side has the opposite direction. From the direction of the vortices on both sides of the airfoil, we can see that they also create a downward flow. We can also see that these vortices are colliding with the following airfoil in this visualization.

ICCS Camera Ready Version 2022
To cite this paper please use the final published version:
DOI: 10.1007/978-3-031-08760-8_27

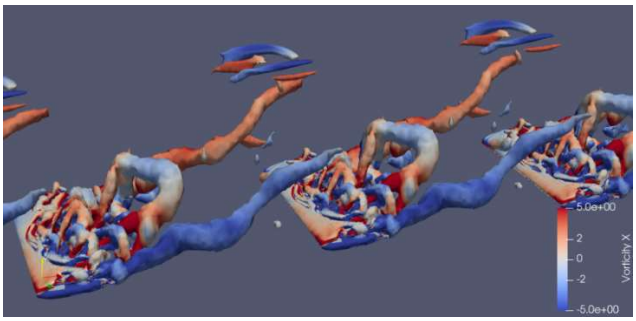

Fig. 4. Isosurfaces of Q criterion where the airfoils are descending at the frequency 0.2Hz. In this figure, a single calculation result is displayed in a row to represent the infinite array of the airfoils. The figure is colored by the x component (stream-wise) of vorticity.

4 Conclusion

The model of Becker et al. to analyze bird and fish schools was reproduced to a limited extent in 3D unsteady simulations. It was found that the travel speeds of the model obtained from simulations using the airfoils corresponded to the experimental values. As for the flow field, it was found that the upward and downward flows generated by the airfoil affected the propulsion of the airfoil as in the experiment. In addition, the structure of the wake generated by the airfoil was clarified by visualizing the flow. Unlike the two-dimensional simulation in [3], it was found that the vortices facing the direction of the airfoil also contributed to the formation of the upward and downward flows.

For future works, we will conduct this unsteady three-dimensional simulation in a wide range of the flapping frequency and clarify the characteristics of the infinite array of the airfoils.

Acknowledgements

This publication was subsidized by JKA through its promotion funds from KEIRIN RACE and by JSPS KAKENHI Grant Number 21K03856.

References

1. Wu X, Zhang X, Tian X, Li X, Lu W (2020) A review on fluid dynamics of flapping foils. Ocean Engineering 195:106712 . https://doi.org/10.1016/j.oceaneng.2019.106712

2. Weihs D (1973) Hydromechanics of Fish Schooling. Nature 241:290–291 . https://doi.org/10.1038/241290a0

ICCS Camera Ready Version 2022
To cite this paper please use the final published version:
DOI: 10.1007/978-3-031-08760-8_27

3. Becker AD, Masoud H, Newbolt JW, Shelley M, Ristroph L (2015) Hydrodynamic schooling of flapping swimmers. Nat Commun 6:8514 . https://doi.org/10.1038/ncomms9514

4. Mihara K, Matsuno K, Satofuka N (1999) An Iterative Finite-Volume Scheme on a Moving Grid : 1st Report, The Fundamental Formulation and Validation. Transactions of the Japan Society of Mechanical Engineers Series B 65:2945–2953 . https://doi.org/10.1299/kikaib.65.2945

5. Inomoto T, Matsuno K, Yamakawa M (2013) 303 Unstructured Moving-Grid Finite-Volume Method for Incompressible Flows. The Proceedings of The Computational Mechanics Conference 2013.26:_303-1_-_303-2_ . https://doi.org/10.1299/jsmecmd.2013.26._303-1_

6. Watanabe K, Matsuno K (2009) Moving Computational Domain Method and Its Application to Flow Around a High-Speed Car Passing Through a Hairpin Curve. JCST 3:449–459 . https://doi.org/10.1299/jcst.3.449

7. Kim J, Moin P (1985) Application of a fractional-step method to incompressible Navier-Stokes equations. Journal of Computational Physics 59:308–323 . https://doi.org/10.1016/0021-9991(85)90148-2

8. Yoon S, Jameson A (1988) Lower-upper Symmetric-Gauss-Seidel method for the Euler and Navier-Stokes equations. AIAA Journal 26:1025–1026 . https://doi.org/10.2514/3.10007

9. Ito Y (2013) Challenges in unstructured mesh generation for practical and efficient computational fluid dynamics simulations. Computers & Fluids 85:47–52

10. Vandenberghe N, Zhang J, Childress S (2004) Symmetry breaking leads to forward flapping flight. J Fluid Mech 506:147–155. https://doi.org/10.1017/S0022112004008468

11. Jeong J, Hussain F (1995) Hussain, F.: On the identification of a vortex. JFM 285,69-94.Journal of Fluid Mechanics 285:69–94. https://doi.org/10.1017/S0022112095000462

ICCS Camera Ready Version 2022
To cite this paper please use the final published version:
DOI: 10.1007/978-3-031-08760-8_27